Measurement of the direct CP violating charge asymmetry in $B^\pm \to \mu^\pm \nu_\mu D^0$ decays

V.M. Abazov,[31] B. Abbott,[67] B.S. Acharya,[25] M. Adams,[46] T. Adams,[44] J.P. Agnew,[41] G.D. Alexeev,[31]
G. Alkhazov,[35] A. Alton[a],[56] A. Askew,[44] S. Atkins,[54] K. Augsten,[7] V. Aushev,[38] Y. Aushev,[38] C. Avila,[5]
F. Badaud,[10] L. Bagby,[45] B. Baldin,[45] D.V. Bandurin,[74] S. Banerjee,[25] E. Barberis,[55] P. Baringer,[53] J.F. Bartlett,[45]
U. Bassler,[15] V. Bazterra,[46] A. Bean,[53] M. Begalli,[2] L. Bellantoni,[45] S.B. Beri,[23] G. Bernardi,[14] R. Bernhard,[19]
I. Bertram,[39] M. Besançon,[15] R. Beuselinck,[40] P.C. Bhat,[45] S. Bhatia,[58] V. Bhatnagar,[23] G. Blazey,[47] S. Blessing,[44]
K. Bloom,[59] A. Boehnlein,[45] D. Boline,[64] E.E. Boos,[33] G. Borissov,[39] M. Borysova[l],[38] A. Brandt,[71] O. Brandt,[20]
M. Brochmann,[75] R. Brock,[57] A. Bross,[45] D. Brown,[14] X.B. Bu,[45] M. Buehler,[45] V. Buescher,[21] V. Bunichev,[33]
S. Burdin[b],[39] C.P. Buszello,[37] E. Camacho-Pérez,[28] B.C.K. Casey,[45] H. Castilla-Valdez,[28] S. Caughron,[57]
S. Chakrabarti,[64] K.M. Chan,[51] A. Chandra,[73] E. Chapon,[15] G. Chen,[53] S.W. Cho,[27] S. Choi,[27] B. Choudhary,[24]
S. Cihangir[‡],[45] D. Claes,[59] J. Clutter,[53] M. Cooke[k],[45] W.E. Cooper,[45] M. Corcoran,[73] F. Couderc,[15]
M.-C. Cousinou,[12] J. Cuth,[21] D. Cutts,[70] A. Das,[72] G. Davies,[40] S.J. de Jong,[29, 30] E. De La Cruz-Burelo,[28]
F. Déliot,[15] R. Demina,[63] D. Denisov,[45] S.P. Denisov,[34] S. Desai,[45] C. Deterre[c],[41] K. DeVaughan,[59] H.T. Diehl,[45]
M. Diesburg,[45] P.F. Ding,[41] A. Dominguez,[59] A. Dubey,[24] L.V. Dudko,[33] A. Duperrin,[12] S. Dutt,[23] M. Eads,[47]
D. Edmunds,[57] J. Ellison,[43] V.D. Elvira,[45] Y. Enari,[14] H. Evans,[49] A. Evdokimov,[46] V.N. Evdokimov,[34]
A. Fauré,[15] L. Feng,[47] T. Ferbel,[63] F. Fiedler,[21] F. Filthaut,[29, 30] W. Fisher,[57] H.E. Fisk,[45] M. Fortner,[47]
H. Fox,[39] J. Franc,[7] S. Fuess,[45] P.H. Garbincius,[45] A. Garcia-Bellido,[63] J.A. García-González,[28] V. Gavrilov,[32]
W. Geng,[12, 57] C.E. Gerber,[46] Y. Gershtein,[60] G. Ginther,[45] O. Gogota,[38] G. Golovanov,[31] P.D. Grannis,[64]
S. Greder,[16] H. Greenlee,[45] G. Grenier,[17] Ph. Gris,[10] J.-F. Grivaz,[13] A. Grohsjean[c],[15] S. Grünendahl,[45]
M.W. Grünewald,[26] T. Guillemin,[13] G. Gutierrez,[45] P. Gutierrez,[67] J. Haley,[68] L. Han,[4] K. Harder,[41] A. Harel,[63]
J.M. Hauptman,[52] J. Hays,[40] T. Head,[41] T. Hebbeker,[18] D. Hedin,[47] H. Hegab,[68] A.P. Heinson,[43] U. Heintz,[70]
C. Hensel,[1] I. Heredia-De La Cruz[d],[28] K. Herner,[45] G. Hesketh[f],[41] M.D. Hildreth,[51] R. Hirosky,[74] T. Hoang,[44]
J.D. Hobbs,[64] B. Hoeneisen,[9] J. Hogan,[73] M. Hohlfeld,[21] J.L. Holzbauer,[58] I. Howley,[71] Z. Hubacek,[7, 15]
V. Hynek,[7] I. Iashvili,[62] Y. Ilchenko,[72] R. Illingworth,[45] A.S. Ito,[45] S. Jabeen[m],[45] M. Jaffré,[13] A. Jayasinghe,[67]
M.S. Jeong,[27] R. Jesik,[40] P. Jiang[‡],[4] K. Johns,[42] E. Johnson,[57] M. Johnson,[45] A. Jonckheere,[45] P. Jonsson,[40]
J. Joshi,[43] A.W. Jung[o],[45] A. Juste,[36] E. Kajfasz,[12] D. Karmanov,[33] I. Katsanos,[59] M. Kaur,[23] R. Kehoe,[72]
S. Kermiche,[12] N. Khalatyan,[45] A. Khanov,[68] A. Kharchilava,[62] Y.N. Kharzheev,[31] I. Kiselevich,[32] J.M. Kohli,[23]
A.V. Kozelov,[34] J. Kraus,[58] A. Kumar,[62] A. Kupco,[8] T. Kurča,[17] V.A. Kuzmin,[33] S. Lammers,[49] P. Lebrun,[17]
H.S. Lee,[27] S.W. Lee,[52] W.M. Lee,[45] X. Lei,[42] J. Lellouch,[14] D. Li,[14] H. Li,[74] L. Li,[43] Q.Z. Li,[45] J.K. Lim,[27]
D. Lincoln,[45] J. Linnemann,[57] V.V. Lipaev[‡],[34] R. Lipton,[45] H. Liu,[72] Y. Liu,[4] A. Lobodenko,[35] M. Lokajicek,[8]
R. Lopes de Sa,[45] R. Luna-Garcia[g],[28] A.L. Lyon,[45] A.K.A. Maciel,[1] R. Madar,[19] R. Magaña-Villalba,[28]
S. Malik,[59] V.L. Malyshev,[31] J. Mansour,[20] J. Martínez-Ortega,[28] R. McCarthy,[64] C.L. McGivern,[41]
M.M. Meijer,[29, 30] A. Melnitchouk,[45] D. Menezes,[47] P.G. Mercadante,[3] M. Merkin,[33] A. Meyer,[18] J. Meyer[i],[20]
F. Miconi,[16] N.K. Mondal,[25] M. Mulhearn,[74] E. Nagy,[12] M. Narain,[70] R. Nayyar,[42] H.A. Neal,[56] J.P. Negret,[5]
P. Neustroev,[35] H.T. Nguyen,[74] T. Nunnemann,[22] J. Orduna,[70] N. Osman,[12] A. Pal,[71] N. Parashar,[50]
V. Parihar,[70] S.K. Park,[27] R. Partridge[e],[70] N. Parua,[49] A. Patwa[j],[65] B. Penning,[40] M. Perfilov,[33]
Y. Peters,[41] K. Petridis,[41] G. Petrillo,[63] P. Pétroff,[13] M.-A. Pleier,[65] V.M. Podstavkov,[45] A.V. Popov,[34]
M. Prewitt,[73] D. Price,[41] N. Prokopenko,[34] J. Qian,[56] A. Quadt,[20] B. Quinn,[58] P.N. Ratoff,[39] I. Razumov,[34]
I. Ripp-Baudot,[16] F. Rizatdinova,[68] M. Rominsky,[45] A. Ross,[39] C. Royon,[8] P. Rubinov,[45] R. Ruchti,[51] G. Sajot,[11]
A. Sánchez-Hernández,[28] M.P. Sanders,[22] A.S. Santos[h],[1] G. Savage,[45] M. Savitskyi,[38] L. Sawyer,[54]
T. Scanlon,[40] R.D. Schamberger,[64] Y. Scheglov,[35] H. Schellman,[69, 48] M. Schott,[21] C. Schwanenberger,[41]
R. Schwienhorst,[57] J. Sekaric,[53] H. Severini,[67] E. Shabalina,[20] V. Shary,[15] S. Shaw,[41] A.A. Shchukin,[34] O. Shkola,[38]
V. Simak,[7] P. Skubic,[67] P. Slattery,[63] G.R. Snow,[59] J. Snow,[66] S. Snyder,[65] S. Söldner-Rembold,[41]
L. Sonnenschein,[18] K. Soustruznik,[6] J. Stark,[11] N. Stefaniuk,[38] D.A. Stoyanova,[34] M. Strauss,[67] L. Suter,[41]
P. Svoisky,[74] M. Titov,[15] V.V. Tokmenin,[31] Y.-T. Tsai,[63] D. Tsybychev,[64] B. Tuchming,[15] C. Tully,[61]
L. Uvarov,[35] S. Uvarov,[35] S. Uzunyan,[47] R. Van Kooten,[49] W.M. van Leeuwen,[29] N. Varelas,[46] E.W. Varnes,[42]
I.A. Vasilyev,[34] A.Y. Verkheev,[31] L.S. Vertogradov,[31] M. Verzocchi,[45] M. Vesterinen,[41] D. Vilanova,[15] P. Vokac,[7]
H.D. Wahl,[44] M.H.L.S. Wang,[45] J. Warchol,[51] G. Watts,[75] M. Wayne,[51] J. Weichert,[21] L. Welty-Rieger,[48]
M.R.J. Williams[n],[49] G.W. Wilson,[53] M. Wobisch,[54] D.R. Wood,[55] T.R. Wyatt,[41] Y. Xie,[45] R. Yamada,[45]
S. Yang,[4] T. Yasuda,[45] Y.A. Yatsunenko,[31] W. Ye,[64] Z. Ye,[45] H. Yin,[45] K. Yip,[65] S.W. Youn,[45] J.M. Yu,[56]

J. Zennamo,[62] T.G. Zhao,[41] B. Zhou,[56] J. Zhu,[56] M. Zielinski,[63] D. Zieminska,[49] and L. Zivkovic[p14]

(The D0 Collaboration)

[1]*LAFEX, Centro Brasileiro de Pesquisas Físicas, Rio de Janeiro, RJ 22290, Brazil*
[2]*Universidade do Estado do Rio de Janeiro, Rio de Janeiro, RJ 20550, Brazil*
[3]*Universidade Federal do ABC, Santo André, SP 09210, Brazil*
[4]*University of Science and Technology of China, Hefei 230026, People's Republic of China*
[5]*Universidad de los Andes, Bogotá, 111711, Colombia*
[6]*Charles University, Faculty of Mathematics and Physics,*
Center for Particle Physics, 116 36 Prague 1, Czech Republic
[7]*Czech Technical University in Prague, 116 36 Prague 6, Czech Republic*
[8]*Institute of Physics, Academy of Sciences of the Czech Republic, 182 21 Prague, Czech Republic*
[9]*Universidad San Francisco de Quito, Quito, Ecuador*
[10]*LPC, Université Blaise Pascal, CNRS/IN2P3, Clermont, F-63178 Aubière Cedex, France*
[11]*LPSC, Université Joseph Fourier Grenoble 1, CNRS/IN2P3,*
Institut National Polytechnique de Grenoble, F-38026 Grenoble Cedex, France
[12]*CPPM, Aix-Marseille Université, CNRS/IN2P3, F-13288 Marseille Cedex 09, France*
[13]*LAL, Univ. Paris-Sud, CNRS/IN2P3, Université Paris-Saclay, F-91898 Orsay Cedex, France*
[14]*LPNHE, Universités Paris VI and VII, CNRS/IN2P3, F-75005 Paris, France*
[15]*CEA Saclay, Irfu, SPP, F-91191 Gif-Sur-Yvette Cedex, France*
[16]*IPHC, Université de Strasbourg, CNRS/IN2P3, F-67037 Strasbourg, France*
[17]*IPNL, Université Lyon 1, CNRS/IN2P3, F-69622 Villeurbanne Cedex,*
France and Université de Lyon, F-69361 Lyon CEDEX 07, France
[18]*III. Physikalisches Institut A, RWTH Aachen University, 52056 Aachen, Germany*
[19]*Physikalisches Institut, Universität Freiburg, 79085 Freiburg, Germany*
[20]*II. Physikalisches Institut, Georg-August-Universität Göttingen, 37073 Göttingen, Germany*
[21]*Institut für Physik, Universität Mainz, 55099 Mainz, Germany*
[22]*Ludwig-Maximilians-Universität München, 80539 München, Germany*
[23]*Panjab University, Chandigarh 160014, India*
[24]*Delhi University, Delhi-110 007, India*
[25]*Tata Institute of Fundamental Research, Mumbai-400 005, India*
[26]*University College Dublin, Dublin 4, Ireland*
[27]*Korea Detector Laboratory, Korea University, Seoul, 02841, Korea*
[28]*CINVESTAV, Mexico City 07360, Mexico*
[29]*Nikhef, Science Park, 1098 XG Amsterdam, the Netherlands*
[30]*Radboud University Nijmegen, 6525 AJ Nijmegen, the Netherlands*
[31]*Joint Institute for Nuclear Research, Dubna 141980, Russia*
[32]*Institute for Theoretical and Experimental Physics, Moscow 117259, Russia*
[33]*Moscow State University, Moscow 119991, Russia*
[34]*Institute for High Energy Physics, Protvino, Moscow region 142281, Russia*
[35]*Petersburg Nuclear Physics Institute, St. Petersburg 188300, Russia*
[36]*Institució Catalana de Recerca i Estudis Avançats (ICREA) and Institut*
de Física d'Altes Energies (IFAE), 08193 Bellaterra (Barcelona), Spain
[37]*Uppsala University, 751 05 Uppsala, Sweden*
[38]*Taras Shevchenko National University of Kyiv, Kiev, 01601, Ukraine*
[39]*Lancaster University, Lancaster LA1 4YB, United Kingdom*
[40]*Imperial College London, London SW7 2AZ, United Kingdom*
[41]*The University of Manchester, Manchester M13 9PL, United Kingdom*
[42]*University of Arizona, Tucson, Arizona 85721, USA*
[43]*University of California Riverside, Riverside, California 92521, USA*
[44]*Florida State University, Tallahassee, Florida 32306, USA*
[45]*Fermi National Accelerator Laboratory, Batavia, Illinois 60510, USA*
[46]*University of Illinois at Chicago, Chicago, Illinois 60607, USA*
[47]*Northern Illinois University, DeKalb, Illinois 60115, USA*
[48]*Northwestern University, Evanston, Illinois 60208, USA*
[49]*Indiana University, Bloomington, Indiana 47405, USA*
[50]*Purdue University Calumet, Hammond, Indiana 46323, USA*
[51]*University of Notre Dame, Notre Dame, Indiana 46556, USA*
[52]*Iowa State University, Ames, Iowa 50011, USA*
[53]*University of Kansas, Lawrence, Kansas 66045, USA*
[54]*Louisiana Tech University, Ruston, Louisiana 71272, USA*
[55]*Northeastern University, Boston, Massachusetts 02115, USA*
[56]*University of Michigan, Ann Arbor, Michigan 48109, USA*
[57]*Michigan State University, East Lansing, Michigan 48824, USA*

[58] *University of Mississippi, University, Mississippi 38677, USA*
[59] *University of Nebraska, Lincoln, Nebraska 68588, USA*
[60] *Rutgers University, Piscataway, New Jersey 08855, USA*
[61] *Princeton University, Princeton, New Jersey 08544, USA*
[62] *State University of New York, Buffalo, New York 14260, USA*
[63] *University of Rochester, Rochester, New York 14627, USA*
[64] *State University of New York, Stony Brook, New York 11794, USA*
[65] *Brookhaven National Laboratory, Upton, New York 11973, USA*
[66] *Langston University, Langston, Oklahoma 73050, USA*
[67] *University of Oklahoma, Norman, Oklahoma 73019, USA*
[68] *Oklahoma State University, Stillwater, Oklahoma 74078, USA*
[69] *Oregon State University, Corvallis, Oregon 97331, USA*
[70] *Brown University, Providence, Rhode Island 02912, USA*
[71] *University of Texas, Arlington, Texas 76019, USA*
[72] *Southern Methodist University, Dallas, Texas 75275, USA*
[73] *Rice University, Houston, Texas 77005, USA*
[74] *University of Virginia, Charlottesville, Virginia 22904, USA*
[75] *University of Washington, Seattle, Washington 98195, USA*
(Dated: 2 August 2016, resubmitted 10 January 2017)

We present the first measurement of the CP violating charge asymmetry in $B^{\pm} \to \mu^{\pm} \nu_{\mu} D^0$ decays using the full Run II integrated luminosity of 10.4 fb^{-1} in proton-antiproton collisions collected with the D0 detector at the Fermilab Tevatron Collider. We measure a difference in the yield of B^- and B^+ mesons in these decays by fitting the reconstructed invariant mass distributions. This results in an asymmetry of $A^{\mu D^0} = [-0.14 \pm 0.20]\,\%$, which is consistent with standard model predictions.

I. INTRODUCTION

Direct CP violation (CPV) in the semileptonic decay $B^+ \to \mu^+ \nu_{\mu} \overline{D}^0$ does not occur in the standard model (SM). Any CPV in this decay would indicate the existence of non-SM physics. The anomalously large CP-violating effects in the like-sign dimuon asymmetry measured by the D0 Collaboration [1] could be explained by the presence of direct CPV in semileptonic decays. This article presents the first measurement of the direct CP-violating charge asymmetry. We use the full Run II integrated luminosity of 10.4 fb^{-1} of proton-antiproton collisions collected with the D0 detector at the Fermilab Tevatron Collider. Charge conjugate states are assumed in this paper.

The CPV charge asymmetry is defined as

$$A^{\mu D^0} = \frac{\Gamma(B^- \to \mu^- \overline{\nu}_{\mu} D^0) - \Gamma(B^+ \to \mu^+ \nu_{\mu} \overline{D}^0)}{\Gamma(B^- \to \mu^- \overline{\nu}_{\mu} D^0) + \Gamma(B^+ \to \mu^+ \nu_{\mu} \overline{D}^0)}. \quad (1)$$

We assume that there is no production asymmetry between B^+ and B^- mesons in proton-antiproton collisions and we estimate that any production asymmetry of b baryons and other B mesons that decay to $\mu^+ \overline{D}^0$ is small (see below for further discussion). The measurement is performed using the raw asymmetry

$$A_{\rm raw} = \frac{N_{\mu^- D^0} - N_{\mu^+ \overline{D}^0}}{N_{\mu^- D^0} + N_{\mu^+ \overline{D}^0}}, \quad (2)$$

where $N_{\mu^- D^0}$ ($N_{\mu^+ \overline{D}^0}$) is the number of reconstructed $B^- \to \mu^- \overline{\nu}_{\mu} D^0$ ($B^+ \to \mu^+ \nu_{\mu} \overline{D}^0$) decays. This includes all decay processes of B^+ mesons that result in a D^0 meson and an appropriately charged muon in the final state. Neglecting any terms that are second or higher order in the asymmetry the charge asymmetry in $B^{\pm}$ decays is given by

$$A_{\rm raw} = f_{B^+} A^{\mu D^0} + A_{\rm det} + A_{\rm phys}, \quad (3)$$

where f_{B^+} is fraction of the $\mu^+ \nu_{\mu} \overline{D}^0$ events produced by the decay of a B^+ meson, $A_{\rm det}$ is due to reconstruction asymmetries in the detector, and $A_{\rm phys}$ is the charge asymmetry resulting from the decay of other particles in the sample.

II. DATA SELECTION

The D0 detector has a central tracking system consisting of a silicon microstrip tracker (SMT) and the central fiber tracker (CFT), both located within a 2 T superconducting solenoidal magnet [2, 3]. A muon system, covering $|\eta| < 2$ [4], consists of a layer of tracking detectors and scintillation trigger counters in front of 1.8 T toroidal iron magnets, followed by two similar layers after the toroids [5].

The polarities of the toroidal and solenoidal magnetic fields are reversed on average every two weeks so that the four solenoid-toroid polarity combinations are exposed to approximately the same integrated luminosity. This allows for a cancellation of first-order effects related to instrumental charge and momentum reconstruction asymmetries. To ensure a more complete cancellation of the

uncertainties, the events are weighted according to the number of $\mu^+\nu_\mu\overline{D}^0$ decays collected in each configuration of the magnet polarities (polarity weighting). The weighting is based on the number of events containing D^0 decay products that pass the selection criteria and the likelihood selection (described below), and that are in the $K^+\pi^-$ invariant mass range used for the fit.

The data are collected with a suite of single and dimuon triggers. B^+ mesons are selected using their semileptonic decays $B^+ \to \mu^+\nu_\mu\overline{D}^0$ by applying criteria similar to those used in Ref. [6]. Muons are required to have hits in more than one muon chamber, an associated track in the central tracking system with hits in both SMT and CFT, transverse momentum $p_T^\mu > 2$ GeV/c as measured in the central tracker, pseudorapidity $|\eta^\mu| < 2$, and total momentum $p^\mu > 3$ GeV/c. The muons that satisfy the selection criteria pass through 12.8 to 14.5 hadronic interaction lengths. The background from hadrons faking muons is negligible.

All charged particles in a given event are clustered into jets using the DURHAM clustering algorithm [7] with the cut-off parameter set to 15 GeV/c. Events with more than one identified muon in the same jet or with a reconstructed $J/\psi \to \mu^+\mu^-$ decays are rejected.

$\overline{D}^0$ candidates are constructed from two tracks of opposite sign of curvature associated with the same jet as the reconstructed muon. Both tracks are required to have transverse momentum of $p_T > 0.7$ GeV/c. They are required to form a common vertex with a fit $\chi^2 < 16$ for which the number of degrees of freedom (ndof) is 1. The distance d_T^D between the $p\bar{p}$ collision and $\overline{D}^0$ vertices in the transverse plane is required to exceed 3 standard deviations, $d_T^D/\sigma(d_T^D) > 3$. The tracks of the muon and $\overline{D}^0$ candidate must form a common vertex with a fit $\chi^2 < 16$ (ndof = 1). The mass of the kaon is assigned to the track having the same sign of curvature as the muon. The remaining track is assigned the mass of the charged pion. The mass of the $\mu^+\overline{D}^0$ system is required to be $2.0 < M(\mu^+\overline{D}^0) < 5.5$ GeV/c^2. The distance d_T^B between the $p\bar{p}$ collision and B vertices in the transverse plane must be $> 3\sigma(d_T^B)$.

The $K^\pm\pi^\mp$ mass distribution for the selected sample and the results of the fit to signal and background components are shown in Fig. 1.

III. RAW ASYMMETRY

We choose a fitting function to give a good representation of the $K^+\pi^-$ mass spectrum over the entire sample of $\mu^+\nu_\mu\overline{D}^0$ polarity weighted events shown in Fig. 1.

The signal peak corresponding to the decay $\overline{D}^0 \to K^+\pi^-$ lies at $M(K^\pm\pi^\mp) = 1.857$ GeV/c^2. The background in the mass region above the signal is adequately described
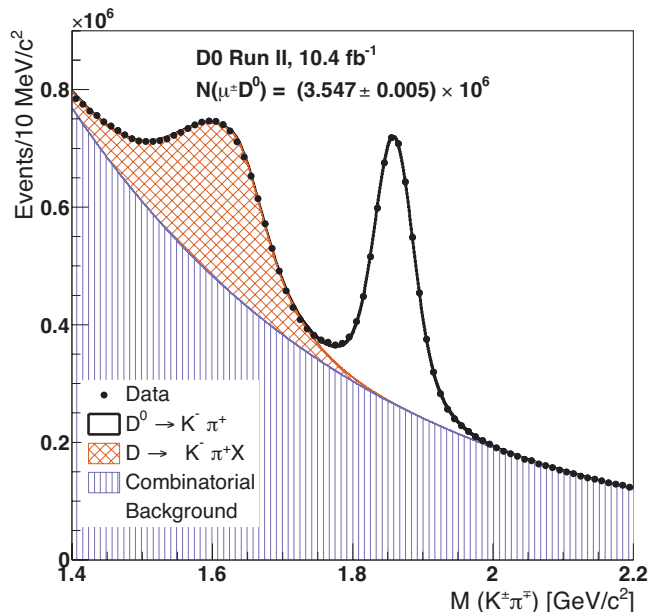

FIG. 1. The sum of the $K^+\pi^-$ and $K^-\pi^+$ invariant mass distributions for selected μD^0 candidates. The curve shows the result of the fit described in the text.

by an exponential function in the $K\pi$ mass M:

$$f_1^{\rm bkg}(M) = \exp\left(a_0 - a_1 M\right), \qquad (4)$$

where a_0 and a_1 are fit parameters.

The signal is modelled by the sum of two Gaussians:

$$f^{\rm sig}(M) = \frac{N^{\rm sig}}{\sqrt{2\pi}}\left[\frac{r_1}{\sigma_1}\exp\left(-\frac{(M - M_{D^0})^2}{2\sigma_1^2}\right)\right.$$
$$\left. + \frac{1 - r_1}{\sigma_2}\exp\left(-\frac{(M - M_{D^0})^2}{2\sigma_2^2}\right)\right], \quad (5)$$

where $N^{\rm sig}$ is the number of signal events, M_{D^0} is the mean of the Gaussian functions, σ_1 and σ_2 are their widths, and r_1 is the fractional contribution of the first Gaussian function.

The peak in the background below the signal region is due to D mesons decaying to $K^+\pi^-X$, where X is not reconstructed (X is typically a π^0). It is modelled with a bifurcated Gaussian function:

$$f_2^{\mathrm{bkg}}(M) = N_2 \left[r_1 \exp\left(-\frac{(M-\mu_0)^2}{2\sigma_R^2}\right) + (1-r_1)\exp\left(-\frac{(M-\mu_0)^2}{2(S\sigma_R)^2}\right)\right] \quad \text{for} \quad M-\mu_0 \geq 0,$$
$$= N_2 \left[r_1 \exp\left(-\frac{(M-\mu_0)^2}{2\sigma_L^2}\right) + (1-r_1)\exp\left(-\frac{(M-\mu_0)^2}{2(S\sigma_L)^2}\right)\right] \quad \text{for} \quad M-\mu_0 < 0. \quad (6)$$

Here, μ_0 is the mean of the Gaussian function, σ_L and σ_R are the two widths of the bifurcated Gaussian function, r_1 is the fractional contribution of the first Gaussian function which is constrained to be the same as the fraction in the signal peak, and $S = \sigma_2/\sigma_1$ from the fitted signal peak (Eq. 5). These constraints are a result of the detector mass resolution and are required for the fit to converge.

The fit yields $(3.547 \pm 0.005) \times 10^6$ $\mu^+\overline{D}^0$ candidates. The raw asymmetry (Eq. 2) is extracted by fitting the $K^+\pi^-$ mass spectrum using a χ^2 minimization. The fit is performed simultaneously, using the same model, on the sum (Fig. 1) and the difference (Fig. 2) of the $M(K^-\pi^+)$ distribution for the μ^-D^0 candidates and the $M(K^+\pi^-)$ distribution for the $\mu^+\overline{D}^0$ candidates. The functions used to model the two distributions are

$$f_{\mathrm{sum}}(M) = f^{\mathrm{sig}}(M) + f_1^{\mathrm{bkg}}(M) + f_2^{\mathrm{bkg}}(M), \quad (7)$$
$$f_{\mathrm{diff}}(M) = A_{\mathrm{raw}}f^{\mathrm{sig}}(M) + A_1 f_1^{\mathrm{bkg}}(M) + A_2 f_2^{\mathrm{bkg}}(M). \quad (8)$$

Here, A_1 is the asymmetry of the combinatoric background, and A_2 is the asymmetry of the $\overline{D}$ mesons that decay to $K^+\pi^-X$, where X is not reconstructed. The fitted asymmetry parameters are $A_{\mathrm{raw}} = (-1.12 \pm 0.08)\%$, $A_1 = (-0.50\pm0.03)\%$ and $A_2 = (-0.87\pm0.12)\%$ (Fig. 2) where the uncertainties are statistical.

Systematic uncertainties on the fitting method are evaluated by varying the fitting procedure. The mass range of the fit is shifted from $1.40 < M < 2.20$ GeV/c^2 to $1.43 < M < 2.17$ GeV/c^2 in steps of 10 MeV/c^2. The function modelling the high mass background is changed to a 2nd order polynomial function. The width of the mass bins is varied between 5 and 20 MeV/c^2. The uncertainty for each of these modifications to the fitting procedure is assigned to be half of the maximal variation. The resulting systematic uncertainty is 0.0075% on the raw asymmetry A_{raw}, yielding

$$A_{\mathrm{raw}} = [-1.12 \pm 0.08\,(\mathrm{stat}) \pm 0.008\,(\mathrm{syst})]\,\%. \quad (9)$$

IV. RECONSTRUCTION ASYMMETRIES

The residual reconstruction asymmetries are described in Ref. [8]. The residual detector tracking asymmetry has been studied in Ref. [9] by using $K_S^0 \to \pi^+\pi^-$ and
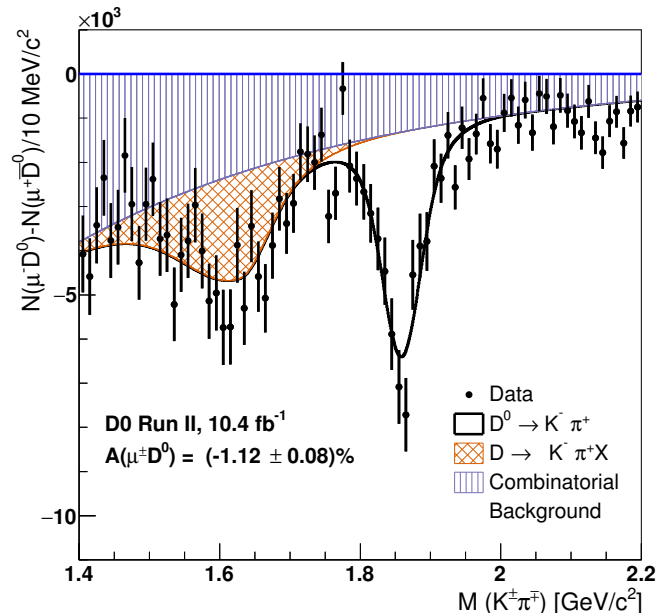

FIG. 2. The results of a fit to the differences between the numbers of μ^-D^0 and $\mu^+\overline{D}^0$ events as function of the $K\pi$ mass.

$K^{*\pm} \to K_S^0\pi^\pm$ decays. These analyses show no significant residual track reconstruction asymmetries in the D0 detector. For this reason no correction for tracking asymmetries is applied ($A_{\mathrm{track}} \equiv 0$). The reconstruction asymmetry of charged pions has been studied using Monte Carlo (MC) simulations of the detector [9]. The asymmetry is found to be less than 0.05% which is assigned as a systematic uncertainty and no correction is made. The muon and the pion have opposite charge, so any remaining track asymmetries will cancel to first order.

The residual reconstruction asymmetry of muons is measured using $J/\psi \to \mu^+\mu^-$ decays as described in [9, 10]. This asymmetry is determined as a function of $p_T(\mu)$ and $|\eta(\mu)|$, and the final correction is obtained by a weighted average over the normalized $(p_T(\mu), |\eta(\mu)|)$ yields, as determined from fits to the $M(K\pi)$ invariant mass distribution. The resulting correction is

$$A_\mu = [\epsilon(\mu^+) - \epsilon(\mu^-)]/[\epsilon(\mu^+) + \epsilon(\mu^-)]$$
$$= [0.10 \pm 0.06\,(\mathrm{syst})]\,\%, \quad (10)$$

where $\epsilon(\mu^\pm)$ are the reconstruction efficiencies of positively and negatively charged muons. This correction

also includes the systematic uncertainty due to track reconstruction.

The correction for a difference in behavior between positively and negatively charged kaons is calculated using the measured kaon reconstruction asymmetry presented in Ref. [8]. Negative kaons can interact with matter to produce hyperons, while there is no equivalent interaction for positive kaons. As a result, the mean path length for positive kaons is larger, the reconstruction efficiency is higher, and the kaon asymmetry A_K is positive.

The kaon asymmetry is measured using a dedicated sample of $K^{*0}(\bar{K}^{*0}) \to K^+\pi^-(K^-\pi^+)$ decays, based on the technique described in Ref. [9]. The $K^+\pi^-$ and $K^-\pi^+$ signal yields are extracted by fitting the charge-specific $M(K^\pm\pi^\mp)$ distributions, and the asymmetry is determined by dividing the difference by the sum of the distributions. The track selection criteria in Ref. [8] are the same as those required in the signal selection in this analysis.

A strong dependence of the kaon asymmetry on kaon momentum $p(K)$ and the absolute value of the pseudorapidity $\eta(K)$ is found. Hence, the final kaon asymmetry correction is determined from the polarity-weighted average of $A_K[p(K), |\eta(K)|]$ over the $p(K)$ and $|\eta(K)|$ distributions in the signal events. A relative systematic uncertainty of 5% is assigned to each bin to account for possible variations in the yield when different models are used to fit the signal and backgrounds in the K^{*0} mass distribution. Based on studies over a range of fit variations the relative systematic uncertainty on the $\mu^+\overline{D}^0$ yields per $p(K)$ and $|\eta(K)|$ bin is 1%. The resulting kaon asymmetry is found to be:

$$A_K = [\epsilon(K^+) - \epsilon(K^-)] / [\epsilon(K^+) + \epsilon(K^-)]$$
$$= [0.92 \pm 0.05\,(\mathrm{syst})]\,\%, \tag{11}$$

where $\epsilon(K^\pm)$ is the reconstruction efficiency of positively and negatively charged kaons.

Combining the detector effects gives

$$A_{\mathrm{det}} = -A_\mu - A_K + A_{\mathrm{track}}$$
$$= [-1.02 \pm 0.08\,(\mathrm{syst})]\,\%. \tag{12}$$

V. SIGNAL COMPOSITION

The fraction of $\mu^+\nu_\mu\overline{D}^0$ events produced by the decay of a B^+ meson, f_{B^+}, is extracted from MC simulations. The $\mu^+\nu_\mu\overline{D}^0$ signal events can also be produced via the decay of B_d^0 mesons, B_s^0 mesons, b baryon decays, and from prompt $\overline{D}^0$ production. We generate a MC sample using the PYTHIA event generator [12] modified to use EVTGEN [13] for the decay of hadrons containing b or c quarks. The PYTHIA inclusive QCD production model is used. Events recorded in random beam crossings are overlaid on the simulated events to quantify the effect of additional collisions in the same or nearby bunch crossings. Events are selected that contain at least one muon

and a $\overline{D}^0 \to K^+\pi^-$ or $D^0 \to K^-\pi^+$ decay. The generated events are processed by the full simulation chain, and then by the same reconstruction and selection algorithms as used to select events from real data.

The mean proper decay lengths of b hadrons are fixed in the simulation to values close to, but not exactly equal to, the current world-average values [11]. To correct for these differences, an event weighting is applied to all non-prompt events in the simulation, based on the generated lifetime of the B candidate, to give the world-average B meson lifetimes. To estimate the effects of the trigger selection and the reconstruction on the data, we weight each event based on the transverse momentum of the reconstructed muon. The combined weighting applied to each MC event i is given by w_i. Combining all of these corrections, we find $f_{B^+} = 0.56$.

The remainder of the events in the signal are semileptonic decays of neutral B mesons ($B_d^0 \to \mu^\pm D^0 X$ and $B_s^0 \to \mu^\pm D^0 X$), the combination of a muon and a D^0 from different sources including prompt production (combinatoric), and hadronic decays of b hadrons where one of the resulting hadrons decays semileptonically $h \to \mu\nu X$ ($B^\pm \to D^0 h$, $B_d^0 \to D^0 h$, $B_s^0 \to D^0 h$, and all other b-hadrons $\to D^0 h$). The sample composition is given in Table I.

TABLE I. Composition and mixing probability of the signal peak determined from MC simulation (the uncertainties are statistical). The total systematic uncertainty on f_{B^+} and the other signal fractions is 0.01.

Decay Type	$P(B_q^0 \to \bar{B}_q^0)$	Fraction
$B^\pm \to \mu^\pm D^0 X$	n/a	$(56.0 \pm 0.2)\%$
$B_d^0 \to \mu^\pm D^0 X^\mp$	0.211	$(35.2 \pm 0.2)\%$
$B_s^0 \to \mu^\pm D^0 X^\mp$	0.5	$(1.8 \pm 0.1)\%$
Combinatoric	n/a	$(0.3 \pm 0.1)\%$
$B^\pm \to D^0 h$	n/a	$(0.9 \pm 0.1)\%$
$B_d^0 \to D^0 h$	0.197	$(5.1 \pm 0.1)\%$
$B_s^0 \to D^0 h$	1.0	$(0 \pm 0.1)\%$
Other b-hadrons $\to D^0 h$	n/a	$(0.7 \pm 0.1)\%$

To determine the systematic uncertainty on f_{B^+}, the exclusive branching ratios and production fractions of B mesons are varied by their uncertainties, the B meson lifetimes are varied within their uncertainties, and a coarser p_T binning is used in the MC event weighting. These variations are combined using a toy MC to determine the size of the systematic uncertainty for the simulation inputs. The total resulting systematic uncertainty on f_{B^+} and the other signal fractions is 0.01.

CP violation in the mixing of neutral B-mesons is a significant background in this analysis. These backgrounds depend on the fraction of neutral B-mesons that have oscillated into their antiparticle prior to decay, $B_q^0 \to \bar{B}_q^0$ or $\bar{B}_q^0 \to B_q^0$ where $q = d, s$. This fraction is given by

$$P(B_q^0 \to \bar{B}_q^0) = \frac{1}{2W} \sum_i w_i \left[1 - \frac{\cos(\Delta m_q t)}{\cosh(0.5\Delta\Gamma_q t)}\right] \tag{13}$$

where Δm_q, and $\Delta \Gamma_q$ are the mass and decay rate differences of the mass eigenstates [11], w_i is the MC event weight and W is the sum of the MC event weights. The fractions for the different B_d^0 and B_s^0 samples are given in Table I. In the case of the B_s^0 meson, the time-integrated oscillation probability is essentially 50% and is insensitive to the exact value of Δm_s. The uncertainties on the mixing fraction are negligible when compared to the uncertainties on the sample composition.

VI. PHYSICS ASYMMETRIES

The most significant potential contribution to A_{phys} is semileptonic charge asymmetries from the mixing of neutral B mesons and is given by

$$A_{B_q^0} = a_{\text{sl}}^q P(B_q^0 \to \bar{B}_q^0) f_{B_q^0} \qquad (14)$$

where $f_{B_q^0}$ is the neutral meson signal fraction. The world average [11] semileptonic charge asymmetry from B_d^0 mixing is $a_{\text{sl}}^d = (-0.15 \pm 0.17)\%$ which would lead to a contribution to A_{phys} of -0.011%. The world average [11] semileptonic charge asymmetry for B_s^0 mixing is $a_{\text{sl}}^s = (-0.75 \pm 0.41)\%$ which would lead to a contribution to A_{phys} of -0.007%. Combining these asymmetries we obtain

$$A_{\text{phys}} = [-0.02 \pm 0.02]\,\%, \qquad (15)$$

where the systematic uncertainty is the combination of uncertainties in the world averages combined with the uncertainties on the sample composition. All other potential asymmetry contributions are assumed to be negligible.

VII. RESULTS

Combining the measured raw asymmetry, and the detector and physics corrections (Eqns 9, 12 and 15) and the estimated B^+ fraction f_{B^+}, we find

$$A^{\mu D^0} = [-0.14 \pm 0.14\,(\text{stat}) \pm 0.14\,(\text{syst})]\,\%. \qquad (16)$$

We can estimate the size of a $B^\pm \to \mu^\pm \nu_\mu D^0$ asymmetry that would be needed to explain the observed like-sign

dimuon asymmetry [1]. The like-sign dimuon asymmetry could be explained by a semileptonic charge asymmetry in neutral B mesons of $A_{\text{sl}}^B \sim 0.5\%$. A MC simulation of same sign dimuon events where one muon originates from a neutral B-meson shows that 62% of these events also contain a muon from a semileptonic B^+ decay. Hence, $0.5\%/0.6 = 0.8\%$ would be required to explain the like-sign dimuon asymmetry. Thus our measurement implies that direct CPV in B^+ decays is unlikely to contribute a significant fraction of the observed dimuon charge asymmetry, and that other explanations need to be sought.

In summary, we have made the first measurement of the direct CP-violating charge asymmetry in B^+ mesons decaying semileptonically to $\mu^+ \nu_\mu \bar{D}^0$. We find $A^{\mu D^0} = [-0.14 \pm 0.14\,(\text{stat}) \pm 0.14\,(\text{syst})]\,\%$ where the total uncertainty is 0.20%. This result is in agreement with the SM expectation of no CPV in this decay.

[1] V. M. Abazov *et al.* (D0 Collaboration), *Study of CP-violating charge asymmetries of single muons and like-sign dimuons in $p\bar{p}$ collisions* Phys. Rev. D **89**, 012002 (2014).
[2] V. M. Abazov *et al.* (D0 Collaboration), *The upgraded D0 detector*, Nucl. Instrum. Methods Phys. Res. A **565**, 463 (2006).
[3] R. Angstadt *et al.*, *The layer 0 inner silicon detector of the D0 experiment*, Nucl. Instrum. Methods Phys. Res. A **622**, 278 (2010).
[4] $\eta = -\ln[\tan(\theta/2)]$ is the pseudorapidity and θ is the polar angle between the track momentum and the proton beam direction. ϕ is the azimuthal angle of the track.
[5] V. M. Abazov *et al.* (D0 Collaboration), *The muon system of the Run II D0 detector*, Nucl. Instrum. Methods Phys. Res. A **552**, 372 (2005).
[6] V. M. Abazov *et al.* (D0 Collaboration), *Measurement of B_d mixing using opposite-side flavor tagging*, Phys. Rev.

D **74**, 112002 (2006).

[7] S. Catani *et al.*, *New clustering algorithm for multijet cross sections in e^+e^- annihilation*, Phys. Lett. B **269**, 432 (1991).

[8] V. M. Abazov *et al.* (D0 Collaboration), *Measurement of the semileptonic charge asymmetry in B^0 meson mixing with the D0 detector*, Phys. Rev. D. **86**, 072009 (2012).

[9] V. M. Abazov *et al.* (D0 Collaboration), *Evidence for an Anomalous Like-Sign Dimuon Charge Asymmetry*, Phys. Rev. D **82**, 032001 (2010); V. M. Abazov *et al.* (D0 Collaboration), *Evidence for an Anomalous Like-Sign Dimuon Charge Asymmetry*, Phys. Rev. Lett. **105**, 081801 (2010).

[10] V. M. Abazov *et al.* (D0 Collaboration), *Measurement of the Anomalous Like-Sign Dimuon Charge Asymmetry with 9 fb^{-1} of $p\bar{p}$ Collisions*, Phys. Rev. **D** 84, 052007 (2011).

[11] C. Patrignani *et al.* (Particle Data Group), *Review of Particle Physics*, Chin. Phys. C, **40**, 100001 (2016)

[12] T. Sjöstrand, S. Mrenna and P. Z. Skands, *PYTHIA 6.4 physics and manual*, J. High Energy Phys. **05**, (2006) 026.

[13] D.G. Lange, *The EvtGen particle decay simulation package*, Nucl. Instrum. Methods Phys. Res. A **462**, 152 (2001); for details see http://www.slac.stanford.edu/~lange/EvtGen.